arXiv:cond-mat/0303170v1 [cond-mat.mes-hall] 10 Mar 2003

Interplay of Short-Range Interactions and Quantum Interference Near the Integer Quantum Hall Transition

V. M. Apalkov and M. E. Raikh
Department of Physics, University of Utah, Salt Lake City, UT 84112, USA

Short-range electron-electron interactions are incorporated into the network model of the integer quantum Hall effect. In the presence of interactions, the electrons, propagating along one link, experience exchange scattering off the Friedel oscillations of the density matrix of electrons on the neighboring links. As a result, the energy dependence of the transmission, $\mathcal{T}(\epsilon)$, of the node, connecting the two links, develops an anomaly at the Fermi level, $\epsilon = \epsilon_F$. We show that this interaction-induced anomaly in $\mathcal{T}(\epsilon)$ translates into the anomalous behavior of the Hall conductivity, $\sigma_{xy}(\nu)$, where ν is the filling factor (we assume that the electrons are *spinless*). At low temperatures, $T \to 0$, the evolution of the quantized σ_{xy} with decreasing ν proceeds as $1 \to 2 \to 0$, in apparent violation of the semicircle relation. The anomaly in $\mathcal{T}(\epsilon)$ also affects the temperature dependence of the peak in the diagonal conductivity, $\sigma_{xx}(\nu, T)$. In particular, unlike the case of noninteracting electrons, the maximum value of σ_{xx} stays at $\sigma_{xx} = 0.5$ within a wide temperature interval.

I. INTRODUCTION

Understanding of the integer quantum Hall transitions was strongly facilitated by the network model [1] introduced by Chalker and Coddington (CC). Within this model, delocalization of single-electron states at certain discrete energies is governed by quantum interference of waves, propagating along the chiral links connecting the nodes of the network. In contrast to the original network model [2], the CC model emerges in a natural way from the microscopic consideration of an electron moving in a smooth potential, $U(x, y)$, and a strong perpendicular magnetic field. Then the chiral links of the network are nothing but the equipotential lines, $U(x, y) = const$. This semiclassical picture corresponds to the case when the magnitude of the random potential, U_0, is much less than the cyclotron energy, while the correlation radius, R_c, is much bigger than the magnetic length, l. The interference effects become important within the energy interval

$$\Gamma = U_0 \left(\frac{l}{R_c} \right)^2 \tag{1}$$

around the center of the Landau band. Since $\Gamma \ll U_0$, the "unit cell" of the CC network has a characteristic size $D_c = R_c(U_0/\Gamma)^{4/3}$, as follows from the percolation theory [3]. The actual lengths of the equipotentials connecting the nodes, which are the saddle points of $U(x, y)$ with heights $\lesssim \Gamma$, are much bigger than D_c, namely, $\mathcal{L}_c \sim R_c(D_c/R_c)^{7/4}$ [3].

On the quantitative level, the CC model yields an accurate value of the critical exponent $\nu_c \approx 7/3$ [4], which governs the divergence of the localization radius, $\xi(\epsilon)$, at small energies $\epsilon \ll \Gamma$, measured from the center of the band

$$\xi(\epsilon) = D_c \left(\frac{\Gamma}{|\epsilon|} \right)^{7/3} . \tag{2}$$

The CC model also yields more delicate characteristics of the transition, such as multifractal exponent of the critical wave functions [5].

The effect of short-range electron-electron interactions on the quantum Hall transition was recently addressed in Ref. [6]. Previously, short-range interactions (*e.g.* screened by a gate) were demonstrated to be irrelevant on the basis of analysis of the renormalization dimension [7]. It was argued in Ref. [6] that, although short-range interactions do not affect the large-distance structure of the critical wave functions [8], they determine the conductance of the quantum Hall sample via the phase breaking time. The underlying physics of the interaction-induced phase breaking in the quantum Hall regime is the same as that for 2D disordered conductor in a zero field [9]. It was shown in Ref. [6] that the exponent, p, in power-law temperature dependence of the phase breaking length, $L_\varphi \propto T^{-p/2}$, is equal to $p = 1.65$ for the interactions screened by a gate. Ref. [6] contains a comprehensive analysis of the temperature and frequency scaling of the conductivity near the transition point. The length L_φ enters into this analysis as a parameter. In short, the current understanding of the transition is based on the assumption that interference effects, responsible for localization, and short-range interactions are effectively *decoupled* from each other.

In this paper we point out that, with short-range interactions, there exists another interaction-related process, qualitatively different from the phase breaking, which is relevant for the quantum Hall transition, namely, the *interaction-induced interference* ($\mathcal{III}$). This process was uncovered by Matveev, Yue, and Glazman [10] in course of the calculation of 1D electron scattering from the point-like impurity in the presence of the Fermi sea. In Ref. [10] a nontrivial interplay between short-range interactions and quantum interference was traced on the microscopic level. Here we generalize the consideration of Ref. [10] to the quantum Hall geometry by incorporating the $\mathcal{III}$ process into the CC model.

We find that strong enough interactions result in the qualitative change in the behavior of the quantized Hall conductivity, σ_{xy}, with increasing magnetic field. In the spinless situation, instead of the transition from e^2/h to the insulator, σ_{xy} undergoes the transitions $1 \to 2 \to 0$. The transition $2 \to 0$ is not accompanied by any change in the diagonal conductivity, σ_{xx}, which remains close to zero, in apparent violation of the semicircle relation [11,12].

We have also studied the impact of $\mathcal{III}$ on the evolution of the σ_{xx} peak with T. It turns out that $\mathcal{III}$ gives rise to an almost metallic behavior at the center of the Landau band, in the sense, that the peak value $\sigma_{xx} = 0.5$ remains temperature-independent within a wide interval of T.

II. INTERACTION-INDUCED INTERFERENCE IN THE QUANTUM HALL REGIME

The original scenario [10] of $\mathcal{III}$ in one dimension is the following. In the absence of interactions, the transformation of an incident wave into reflected and transmitted waves occurs in the vicinity of the impurity. In addition, the impurity causes the Friedel oscillations of the electron density and of the density matrix, which fall off *slowly* at large distances. As the electron-electron interactions are switched on, both perturbations, having the spatial structure with a period $(2k_F)^{-1}$, where k_F is the Fermi momentum, cause the additional coupling of the incident and reflected (from the impurity) electron waves. As a consequence of this coupling, the reflected wave transforms back into the incident wave at distances *far away* from the impurity, and, subsequently, gets transmitted. Interference of this "secondary" transmitted wave, which is due to interactions, with the zero-order transmitted wave is the $\mathcal{III}$ process. Compared to the zero-order transmitted wave, the secondary wave travels an additional closed path, first away from the impurity, and then towards the impurity.

Direct calculation [10] shows that, the $\mathcal{III}$ is constructive, if the coupling between the incident and reflective waves is mediated by the Friedel oscillations of the electron density, and destructive, if it is mediated by the Friedel oscillations of the density matrix. $\mathcal{III}$ is strong, when the energy, ϵ, of the incident electron is close to the Fermi level, ϵ_F. This is due to the Bragg-like resonant enhancement [10], which originates from the fact that the size of the region, where the scattering from the Friedel oscillations takes place, is $\propto |\epsilon - \epsilon_F|^{-1}$. When this size is smaller than the length of the 1D channel, the amplitude of the interaction-induced transmitted wave diverges as $\ln|\epsilon - \epsilon_F|$, indicating that the net transmission is strongly modified by the interactions.

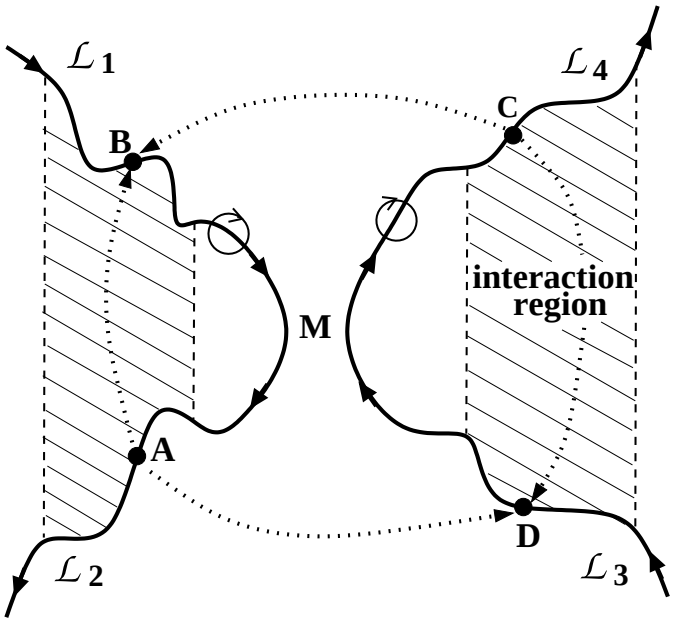

FIG. 1. Schematic illustration a Larmour circle drifting along equipotentials $\mathcal{L}_1$ ...$\mathcal{L}_4$ separated by a saddle point; dotted lines illustrate exchange-induced scattering processes leading to $\mathcal{III}$. This scattering takes place within dashed regions $\sim d$ away from the saddle point.

Let us consider the network model of the quantum Hall effect from the point of view of $\mathcal{III}$. Within the network model, the role of scatterers is played by the saddle points. As it is illustrated in Fig. 1, due to the structure of the saddle-point potential (maximum along the horizontal and minimum along the vertical direction), the electron seas are located only in the dashed regions. Scattering of the electron, drifting along the equipotential line, by the saddle point, differs from the 1D impurity scattering [10] in three respects

(i) Equipotential branches, say, $\mathcal{L}_1$, $\mathcal{L}_2$ *diverge*. Thus, the incident and reflected waves do not interfere far away from the saddle point.

(ii) Starting from short distances, $\mathcal{L}_1$, $\mathcal{L}_2 \gtrsim l$, the electron wave functions, $\Phi_{\mu,\epsilon}(\mathcal{L})$, taken at $\mathcal{L} = \mathcal{L}_1$ and $\mathcal{L} = \mathcal{L}_2$ do not *overlap*. This is because $\Phi_{\mu,\epsilon}(\mathcal{L})$ describe the Landau orbits, drifting along the equipotentials $U(x,y) = \epsilon$; the spatial extent of these functions in the direction normal to the equipotential is $\sim l$. Here the index $\mu = \mathrm{L}, \mathrm{R}$ labels the wave functions incident from the left and from the right, respectively (Fig. 1).

(iii) interaction of an electron incident along $\mathcal{L}_1$ with *both* reflected (drifting along $\mathcal{L}_2$) and transmitted (drifting along $\mathcal{L}_3$) electrons must be taken into account.

The immediate consequence of (ii) is complete absence of the Friedel oscillations of the electron *density*. Thus, the Hartree contribution to the Fermi edge anomaly in 1D impurity scattering, caused by $\mathcal{III}$, is absent in the problem of the reflection from the saddle point. Our prime observation is

that, the contribution, caused by the scattering from the Friedel oscillations of the density matrix (exchange contribution), *survives* in the quantum Hall geometry. To illustrate this, consider the density matrix of electrons drifting along $\mathcal{L}_1$ and $\mathcal{L}_2$

$$\rho\left(\mathcal{L}_2,\mathcal{L}_1\right)=\sum_{\mu}\sum_{\epsilon<\epsilon_F}\Phi^{*}_{\mu,\epsilon}(\mathcal{L}_2)\Phi_{\mu,\epsilon}(\mathcal{L}_1), \tag{3}$$

where, for simplicity, we neglect the spin. If the short-range character of interactions is due to the gate electrode at distance, d, from the 2D plane, then the interaction potential has the form

$$V(\rho)=\frac{e^2}{\kappa}\left[\frac{1}{\rho}-\frac{1}{\sqrt{\rho^2+4d^2}}\right]. \tag{4}$$

The exchange Hamiltonian, acting on the wave function of the electron drifting, say, along equipotential $\mathcal{L}_2$, creates an electron at the point $\mathcal{L}=\mathcal{L}_1$ of the opposite branch, according to the rule

$$\left\{\hat{\mathcal{H}}_{ex}\Phi_{\text{L},\epsilon}\right\}\Big|_{\mathcal{L}=\mathcal{L}_1}=-\int d\mathcal{L}_2 V(\mathcal{L},\mathcal{L}_2)\rho\left(\mathcal{L}_2,\mathcal{L}\right)\Phi_{\text{L},\epsilon}(\mathcal{L}_2), \tag{5}$$

where $V(\mathcal{L}_1,\mathcal{L}_2)$ is the interaction energy of two electrons located at points $\mathcal{L}_1$ and $\mathcal{L}_2$ on different branches. Below we assume that d is much smaller than the period, D_c, of the CC network. Therefore, the contribution to the integral (5) comes only from the piece of equipotential $\mathcal{L}_2$ which lies within the distance $\sim d$ from the saddle point (the actual length of this piece is much bigger than d, see Fig. 1). However, the most important feature of the integral (5) is that, in contrast to the Hartree contribution, the integrand does not contain the product of the wave functions from *different* equipotential branches taken at the *same* point. In other words, the structure of the integrand does not restrict the relative positions of the points $\mathcal{L}$ and $\mathcal{L}_2$ within the magnetic length. In short, the Larmour motion drops out from the exchange contribution, thus making it similar to the 1D case. The integrand in Eq. (5) describes the additional closed-loop contour $A\to B\to M\to A$, traversed by the secondary wave, as illustrated in Fig. 1. Thus we conclude, that III in the quantum Hall geometry is exclusively due to the *indistinguishability* of the electrons.

In contrast to the 1D case, where it diverges logarithmically, the integral (5) *converges*. The reason is that, *on average*, the branches $\mathcal{L}_1$, $\mathcal{L}_2$ depart from each other at large distances. With converging integral (5), there is no need to consider the higher order (in the interaction strength) contributions to the III. By virtue of analogy to the 1D case, the further calculation of the III correction to the transmission coefficient of the saddle point is straightforward.

III. CALCULATION OF THE III CORRECTION

Following Ref. [10], we use Eq. (5) to write down the correction to the wave function, describing the transmitted wave, i.e., the wave propagating along the equipotential $\mathcal{L}_3$ in Fig. 1

$$\delta\Phi_{\text{L},\epsilon}(\mathcal{L}_3)=\delta\Phi_{21}(\mathcal{L}_3)+\delta\Phi_{34}(\mathcal{L}_3)+\delta\Phi_{31}(\mathcal{L}_3)+\delta\Phi_{24}(\mathcal{L}_3), \tag{6}$$

where each term in the r.h.s. corresponds to a certain closed-loop path for the secondary wave. In contrast to the 1D case, where only two paths contribute to the III, there are four possible paths in the quantum Hall geometry (see Fig. 1). The contribution from the path that includes two neighboring equipotentials $\mathcal{L}_i,\mathcal{L}_j$ has the form

$$\delta\Phi_{ij}(\mathcal{L}_3)=-i\pi\int_{\mathcal{L}_i}d\mathcal{L}_i\,\Phi^{*}_{\text{L},\epsilon}(\mathcal{L}_i)\int_{\mathcal{L}_j}d\mathcal{L}_j\,V(\mathcal{L}_i,\mathcal{L}_j)\rho\left(\mathcal{L}_i,\mathcal{L}_j\right)\sum_{\mu}\Phi^{*}_{\mu,\epsilon}(\mathcal{L}_j)\Phi_{\mu,\epsilon}(\mathcal{L}_3) \tag{7}$$

To proceed further, we have to specify the scattering properties of the saddle point
(i) without the loss of generality, we assume that for the function $\Phi_{\text{L},\epsilon}$ of the state, in which the wave, incident along $\mathcal{L}_1$, is reflected into $\mathcal{L}_2$ and transmitted into $\mathcal{L}_3$, the reflection coefficient [13]

$$r_0(\epsilon) = \frac{1}{\left\{1 + \exp\left[\frac{\pi(\epsilon - W)}{\Gamma}\right]\right\}^{1/2}}, \tag{8}$$

and the transmission coefficient, $t_0(\epsilon) = \left[1 - r_0^2(\epsilon)\right]^{1/2}$, are both real. Here $W \lesssim \Gamma$ is the saddle point height.
(ii) away from the saddle point the functional form of the incident wave is $v(\mathcal{L}_1)^{-1/2} \exp\left[i\epsilon\psi(\mathcal{L}_1)\right]$, where $\psi(\mathcal{L})$ is related to the drift velocity $v(\mathcal{L})$ along the equipotential as $d\psi(\mathcal{L})/d\mathcal{L} = v^{-1}(\mathcal{L})$ and $\psi|_{\mathcal{L}=0} = 0$. Substituting this form into Eqs. (3), (7), and then Eq. (7) into Eq. (6), we obtain the following expression for the $\mathcal{III}$ correction to the transmission coefficient

$$\delta t(\epsilon) = -r_0(\epsilon)\left[t_0(\epsilon) r_0(\epsilon_F)\left(I_{21} + I_{34}\right) - t_0(\epsilon_F) r_0(\epsilon)\left(I_{31} + I_{24}\right)\right], \tag{9}$$

where the functions $I_{ij}(\epsilon)$ are defined as

$$I_{ij} = \frac{1}{\pi}\int_0^\infty d\mathcal{L}_i \int_0^\infty d\mathcal{L}_j \left(\frac{V(\mathcal{L}_i, \mathcal{L}_j)}{v(\mathcal{L}_i) v(\mathcal{L}_j)}\right) \frac{\cos\left\{(\epsilon - \epsilon_F)\left[\psi(\mathcal{L}_i) + \psi(\mathcal{L}_j)\right]\right\}}{\psi(\mathcal{L}_i) + \psi(\mathcal{L}_j)}. \tag{10}$$

Note that the last two terms in Eq. (9), originating from the contours $C \to B \to M \to C$ and $A \to D \to M \to A$, that are specific for the quantum Hall geometry, enter with the sign opposite to that of the "conventional" contributions from $A \to B \to M \to A$ and $C \to D \to M \to C$. This fact reflects the unitarity of the scattering matrix of the saddle point. In order to incorporate the correction Eq. (9) into the scattering matrix, we introduce the effective energy according to the rule

$$\mathcal{T}(\epsilon) = |t_0(\epsilon) + \delta t(\epsilon)|^2 = \mathcal{T}_0(\tilde{\epsilon}) = \left\{1 + \exp\left[-\frac{\pi\left(\tilde{\epsilon} - W\right)}{\Gamma}\right]\right\}^{-1}. \tag{11}$$

The meaning of the effective energy, $\tilde{\epsilon}(\epsilon, W)$ is the following. The distribution of the saddle-point heights is even, so that $\langle W \rangle = 0$. The fact that without interactions delocalization occurs at $\epsilon = 0$ can be formally expressed by the condition $\langle(\epsilon - W)\rangle = 0$. Correspondingly, with interactions, the condition for delocalization takes the form $\langle\tilde{\epsilon}(\epsilon, W) - W\rangle = \langle\tilde{\epsilon}(\epsilon, W)\rangle = 0$. From Eq. (11) we obtain for the effective energy

$$\tilde{\epsilon} = \epsilon - \frac{\Gamma}{\pi}\left[\frac{\cosh\frac{\pi(\epsilon - W)}{\Gamma}}{\cosh\frac{\pi(\epsilon_F - W)}{\Gamma}}\right]^{1/2}\left\{\left(I_{21} + I_{34}\right)\exp\left[\frac{\pi(\epsilon - \epsilon_F)}{2\Gamma}\right] - \left(I_{31} + I_{24}\right)\exp\left[\frac{\pi(\epsilon_F - \epsilon)}{2\Gamma}\right]\right\}. \tag{12}$$

Disorder averaging should be performed over the saddle points and over the equipotentials. For energies close to the Fermi level, $|\epsilon - \epsilon_F| \ll \Gamma$ we have $\langle I_{21}\rangle = \langle I_{34}\rangle = \langle I_{31}\rangle = \langle I_{24}\rangle = \mathrm{I}(\epsilon - \epsilon_F)$, so that Eq. (12) takes the form

$$\langle\tilde{\epsilon}(\epsilon)\rangle = \epsilon - (\epsilon - \epsilon_F) I(\epsilon - \epsilon_F), \tag{13}$$

where $I(\epsilon - \epsilon_F)$ is the even function of $(\epsilon - \epsilon_F)$ defined as

$$I(\epsilon - \epsilon_F) = \frac{e^2}{\kappa}\int_0^\infty d\psi_1 \int_0^\infty d\psi_2 \frac{\cos\left\{(\epsilon - \epsilon_F)\left[\psi_1 + \psi_2\right]\right\}}{\psi_1 + \psi_2}\left[\frac{1}{D(\psi_1, \psi_2)} - \frac{1}{\sqrt{D(\psi_1, \psi_2)^2 + 4d^2}}\right]. \tag{14}$$

Eq. (14) emerges upon substituting of the interaction potential (4) into Eq. (10) and introducing the function $D(\psi_1, \psi_2)$, which is the distance between the points, located at neighboring equipotentials, and corresponding to the accumulated phases ψ_1 and ψ_2, respectively. It is easy to see that the integral Eq. (14) contains a contribution from short distances (small ψ), which changes slowly with $(\epsilon - \epsilon_F)$, (characteristic scale $\sim \Gamma$) and a contribution from large distances which is a sharp function of energy. The energy scale, ϵ_0, of this contribution can be estimated from the condition $\epsilon_0 \sim \psi^{-1}$, where ψ is the characteristic phase, for which the distance D is of the order of the distance to the gate, d. Taking into account that D scales with the length, $\mathcal{L}$, along the equipotential as $\mathcal{L}^{4/7}$, we can present the dependence $D(\psi)$ as $D \sim R_c \left(v\psi/R_c\right)^{4/7}$, where v is the characteristic drift velocity. This velocity can be expressed through the parameters of the random potential, i.e., $v \sim U_0 l^2/R_c$, so that $v/R_c \sim \Gamma$ [see Eq. (1)]. Then the condition $D(\epsilon_0^{-1}) = d$ yields

$$\epsilon_0 = \Gamma \left(\frac{R_c}{d}\right)^{7/4} \ll \Gamma. \tag{15}$$

The characteristic magnitude of I follows from Eq. (14) taking into account that the contribution to the integral comes from $\psi_1 \sim \psi_2 \sim \epsilon_0^{-1}$. As a result, Eq. (14) can be presented as

$$I(\epsilon - \epsilon_F) = \alpha \Big[I_0 + F\Big(\frac{\epsilon - \epsilon_F}{\epsilon_0}\Big)\Big], \quad \alpha = \frac{e^2}{\kappa d \Gamma} \left(\frac{d}{R_c}\right)^{7/4}. \tag{16}$$

The contribution $I_0 \sim \ln\left(R_c/l\right)$ comes from small distances, while the asymptotic behavior of the function F is the following

$$F(u)\big|_{u \ll 1} = F_0 - F_1 |u|^{5/7}, \quad F(u)\big|_{u \gg 1} = F_\infty |u|^{-5/7}. \tag{17}$$

With the use of Eq. (16) the expression (13) for the average effective energy takes the form

$$\langle \tilde{\epsilon}(\epsilon) \rangle = \epsilon_F + (\epsilon - \epsilon_F)\Big[(1 - \alpha I_0) - \alpha F\Big(\frac{\epsilon - \epsilon_F}{\epsilon_0}\Big)\Big]. \tag{18}$$

We see that at small $|\epsilon - \epsilon_F| \ll \epsilon_0$ the slope of $\langle \tilde{\epsilon}(\epsilon) \rangle$ can be either positive or negative depending on the sign of $[1 - \alpha\left(I_0 + F_0\right)]$. The consequences of this fact are discussed in the next Section.

IV. IMPLICATIONS

A. $T \to 0$

As was discussed above, the position of a delocalized state can be found from the condition $\langle \tilde{\epsilon}(\epsilon) \rangle = 0$, where $\langle \tilde{\epsilon} \rangle$ is defined by Eq. (18). Interactions enter into this equation via the parameter α. It is easy to see that for $\alpha < \left(I_0 + F_0\right)^{-1}$, i.e., for weak enough interaction strength, the square bracket in the r.h.s of Eq. (18) is always positive. Then it can be easily demonstrated that at any ϵ_F the equation $\langle \tilde{\epsilon}(\epsilon) \rangle = 0$ has only one solution, so that the interactions do not change the scenario of the quantum Hall transition qualitatively. The situation changes as the interaction parameter exceeds the critical value $\alpha_c = \left(I_0 + F_0\right)^{-1}$. For small $(\alpha - \alpha_c) \ll \alpha_c$ the equation $\langle \tilde{\epsilon}(\epsilon) \rangle = 0$ can be analyzed analytically, since the function F in the r.h.s of (18) can be replaced by its small-argument asymptotics Eq. (17). Then we have

$$\langle \tilde{\epsilon}(\epsilon) \rangle = \epsilon_F + (\epsilon - \epsilon_F)\left[\left(1 - \frac{\alpha}{\alpha_c}\right) + \alpha_c F_1 \left|\frac{\epsilon - \epsilon_F}{\epsilon_0}\right|^{5/7}\right] = 0. \tag{19}$$

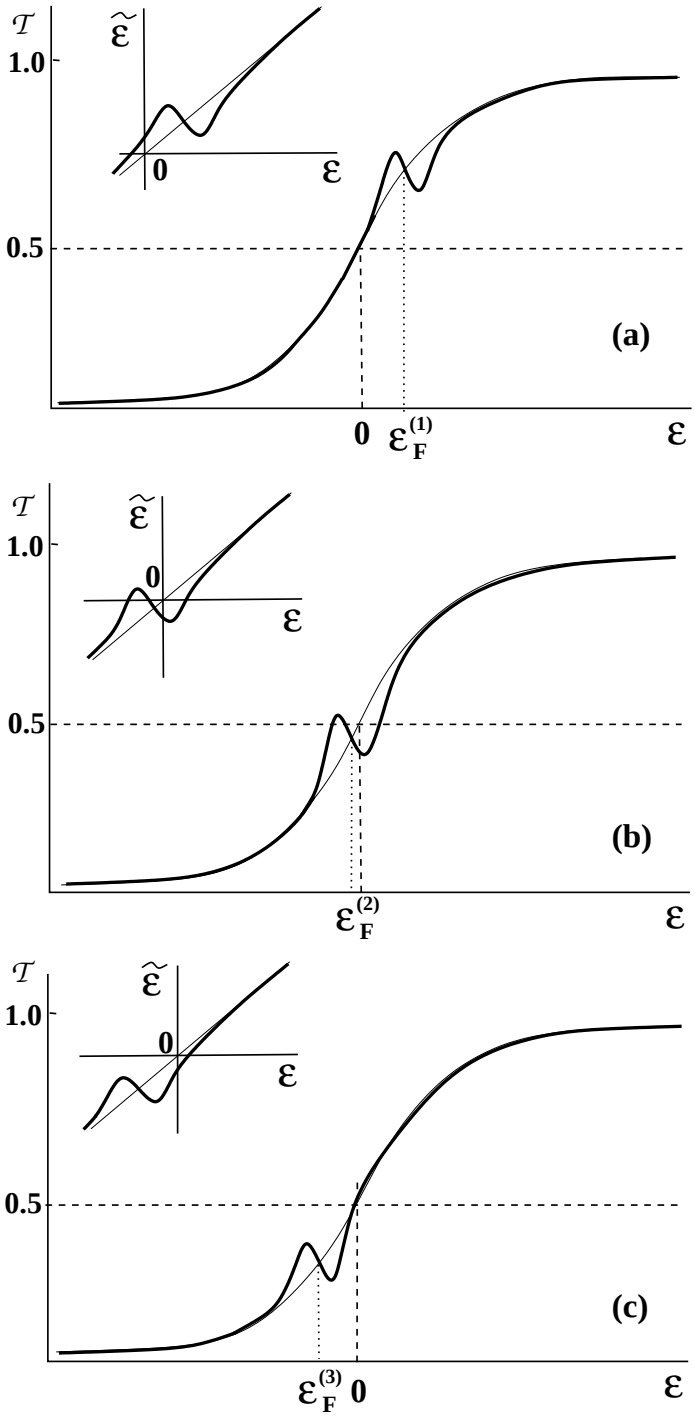

FIG. 2. Energy dependence of the power transmission coefficient, $\mathcal{T}(\epsilon)$, for the interaction strength exceeding the critical value is shown schematically for three positions of the Fermi level, ϵ_F. (a) $\epsilon_F^{(1)} \gg \epsilon_0$; (b) $\epsilon_F^{(2)} \sim \epsilon_0$; (c) $\epsilon_F^{(3)} < 0, \quad |\epsilon_F^{(3)}| \gg \epsilon_0$. Insets show the corresponding energy dependencies of the effective energy, $\tilde{\epsilon}(\epsilon)$, defined by Eq. (11).

Upon introducing a dimensionless variable,

$$Z = \left(\frac{\alpha_c^2 F_1}{\alpha - \alpha_c} \right)^{7/5} \frac{(\epsilon - \epsilon_F)}{\epsilon_0}, \tag{20}$$

Eq. (19) takes the form

$$Z\left(|Z|^{5/7}-1\right)=-\frac{\alpha_c^{19/5}F_1^{7/5}}{(\alpha-\alpha_c)^{12/5}}\left(\frac{\epsilon_F}{\epsilon_0}\right). \tag{21}$$

The l.h.s of Eq. (21) is an odd function of Z and has extrema at $Z=\pm\left(7/12\right)^{7/5}$. Therefore, for ϵ_F within the interval

$$\left|\frac{\epsilon_F}{\epsilon_0}\right|<\frac{5}{7}\left(\frac{7}{12}\right)^{7/5}\frac{(\alpha-\alpha_c)^{12/5}}{\alpha_c^{19/5}F_1^{7/5}} \tag{22}$$

Eq. (21) has *three* solutions. These solutions correspond either to two delocalized states below the Fermi level and one delocalized state above the Fermi level (for $\epsilon_F<0$) or to two delocalized states above the Fermi level and one delocalized state below the Fermi level (for $\epsilon_F>0$). This is quite an unusual situation, since we consider spinless electrons with a filling factor between $\nu=0$ and $\nu=1$. Conventially, as it is the case $\alpha<\alpha_c$, in this situation there is only a single delocalized state. Fig. 2 helps to trace the evolution of the delocalized states with increasing magnetic field. Note first, that, as it follows from Eqs. (11) and (18), for $\alpha>\alpha_c$ the energy dependence of the transmission coefficient, $\mathcal{T}(\epsilon)$, has a region with a negative slope. At low magnetic fields, ($\epsilon_F^{(1)}\gg\epsilon_0$, Fig. 2a) in this region we have $\mathcal{T}(\epsilon)>1/2$. Thus, there is a single delocalized state below the Fermi level. This corresponds to the Hall conductivity $\sigma_{xy}=1$, as in the absence of interactions. The effect of interactions is also negligible at strong magnetic fields ($\epsilon_F^{(3)}<0, |\epsilon_F^{(3)}|\gg\epsilon_0$, Fig. 2c). In this case, the region with negative slope occurs at $\mathcal{T}(\epsilon)<1/2$. A single delocalized state lies above the Fermi level, i.e., $\sigma_{xy}=0$. A nontrivial evolution with magnetic field takes place at small ϵ_F, Fig. 2b. Namely, as Fig. 2a transforms to Fig. 2c with increasing magnetic field, first, in addition to a delocalized state below the Fermi level, *two* delocalized states emerge above the Fermi level. With further increasing magnetic field, the "upper" of two new delocalized states remains above the Fermi level, while the "lower" one moves below the Fermi level. At the critical field when the "lower" delocalized state crosses the Fermi level the diagonal conductivity, σ_{xx}, exhibits a sharp peak, accompanied by a jump of σ_{xy} from $\sigma_{xy}=1$ to $\sigma_{xy}=2$. Two delocalized states below the Fermi level persist within a certain range of magnetic fields, and then disappear abruptly, so that the "normal" arrangement, Fig. 2c, is reinstated. This abrupt disappearance of two delocalized states below the Fermi level manifests itself as a second jump of σ_{xy} from $\sigma_{xy}=2$ to $\sigma_{xy}=0$. Note, that σ_{xx}, which is determined by the states in the immediate vicinity of the Fermi level, remains zero as σ_{xy} experiences a second jump. The evolution of σ_{xy} and σ_{xx} with magnetic field (inverse filling factor) is illustrated in Fig. 3.

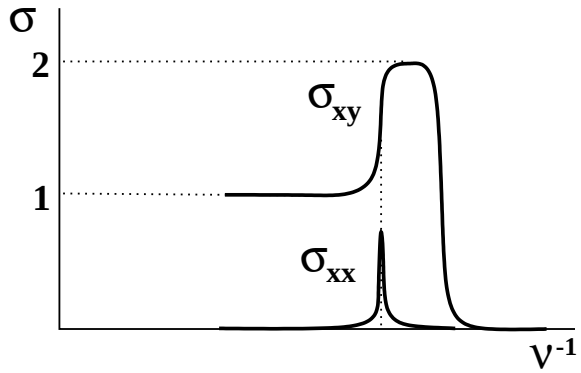

FIG. 3. The components of the conductivity tensor at low temperatures, $T\ll\epsilon_0$, are shown schematically vs. inverse filling factor for the interaction strength exceeding the critical value. Note, that the quantized values of σ_{xy} correspond to *spinless* electrons.

B. "High" T

According to Ref. [6] the temperature dependence of the diagonal conductivity, σ_{xx} of a macroscopic sample can be expressed through the power transmission coefficient, $G(\epsilon, L_\phi)$, of the square of a size L_ϕ calculated for electron with energy ϵ as follows

$$\sigma_{xx} = \frac{1}{2T}\int d\epsilon \left\{\cosh\left(\frac{\epsilon-\epsilon_F}{2T}\right)\right\}^{-2} G\Big[\epsilon, L_\phi\left(T\right)\Big], \tag{23}$$

where $\cosh^{-2}$ comes from the derivative of the Fermi function. The point of Ref. [6] is that the function $G(\epsilon, L_\phi)$ is, in fact, some universal function, $\mathcal{G}_0(X)$, of the argument $X = \Big(L_\phi/\xi\left(\epsilon\right)\Big)^{1/\nu_c}$. The scaling function, $\mathcal{G}_0(X)$, satisfies two conditions
(i) $\mathcal{G}_0(0) = 0.5$, so that at $T \to 0$ Eq. (23) yields $\sigma_{xx} = 0.5$ (in the units of e^2/h).
(ii) $\mathcal{G}_0(X) \sim \exp\left(-c|X|^{\nu_c}\right)$ for $|X| \gg 1$, where $c \sim 1$ is a numerical factor. The latter condition expresses the fact that at short enough ξ the transmission is determined by tunneling, i.e., $|\ln G(\epsilon, L_\phi)| \sim L_\phi/\xi(\epsilon)$. It is convenient to parameterize the temperature dependence of L_ϕ by introducing the characteristic temperature, T_0, via the relation

$$L_\phi(T) = D_c\left(\frac{T}{T_0}\right)^{-p/2}. \tag{24}$$

Using Eq. (24), the condition of applicability of the network model, $L_\phi \gg D_c$, can be presented as $T \ll T_0$. The energies of electrons, contributing to σ_{xx}, are $\sim T$. Therefore, the condition that the network model is adequate within the energy strip, $\epsilon \sim \Gamma$, where the quantum interference is important, reads $T_0 \gg \Gamma$. In the numerical results reported below we measure energies and temperatures in the units of Γ. With localization length given by Eq. (2), the dimensionless argument X takes the form

$$X = \left(\frac{T_0}{\Gamma}\right)^{p/2\nu_c}\left(\frac{T}{\Gamma}\right)^{-p/2\nu_c}\left(\frac{\epsilon}{\Gamma}\right). \tag{25}$$

Consideration in Sect. III suggests that, in the presence of interactions, the energy ϵ in Eq. (25) should be replaced by the effective energy $\tilde{\epsilon}(\epsilon)$ determined by Eq. (13). Below we study how this replacement affects the temperature and magnetic field dependences of σ_{xx} calculated from Eq. (23). For numerical calculations we have chosen the following form of the function $\mathcal{G}_0$

$$\mathcal{G}_0 = \frac{1}{2}\exp\left[1-\left(1+c^{2/\nu_c}X^2\right)^{\nu_c/2}\right]. \tag{26}$$

We have also checked that different forms of $\mathcal{G}_0$, that satisfy the conditions (i) and (ii), change the numerical results only weakly. Upon substituting $\tilde{\epsilon}$ into Eq. (25), then Eq. (25) into Eq. (26), and finally Eq. (26) into Eq. (23), we find that σ_{xx} contains only one unknown parameter, $c^{2/\nu_c}\left(T_0/\Gamma\right)^{p/\nu_c}$, which we have set equal to 2.

In Fig. 4 the calculated dimensionless σ_{xx} as a function of dimensionless magnetic field ϵ_F/Γ is shown for several dimensionless temperatures T/Γ. In Fig. 4a the effect of $\mathcal{III}$ is neglected, i.e., $\tilde{\epsilon} = \epsilon$. In Fig. 4b σ_{xx} is calculated in the presence of $\mathcal{III}$ for $\tilde{\epsilon}(\epsilon)$ dependence shown in the inset. We see that in the absence of $\mathcal{III}$ the broadening of the σ_{xx} peak with increasing T is accompanied by a rapid decrease of the maximal value, $\sigma_{xx}(0) = \sigma_{xx}|_{\epsilon_F=0}$. In particular, at $T/\Gamma = 0.05$, $\sigma_{xx}(0)$ decreases by 20 percent. At the same time, with $\mathcal{III}$ the decrease of $\sigma_{xx}(0)$ at $T/\Gamma = 0.05$ is only 2 percent. The significant drop of $\sigma_{xx}(0)$ by 20 percent occurs only at rather "high" temperature

$T = 0.2\Gamma$. Note, that $\tilde{\epsilon}(\epsilon)$ dependence in Fig. 4b corresponds to the interaction parameter $I(0) = 0.8$ well below the critical value. The drop in $\sigma_{xx}(0)$ with T might seem counterintuitive. It might be argued that the decrease of L_ϕ seems to drive the transport towards fully incoherent regime [11,19], in which the $\sigma_{xx}(0) = 0.5$. However, as it was pointed out in Ref. [6], as a result of the broadening of the Fermi distribution with T, the transmission of the square L_ϕ is almost zero for most of electrons involved in transport.

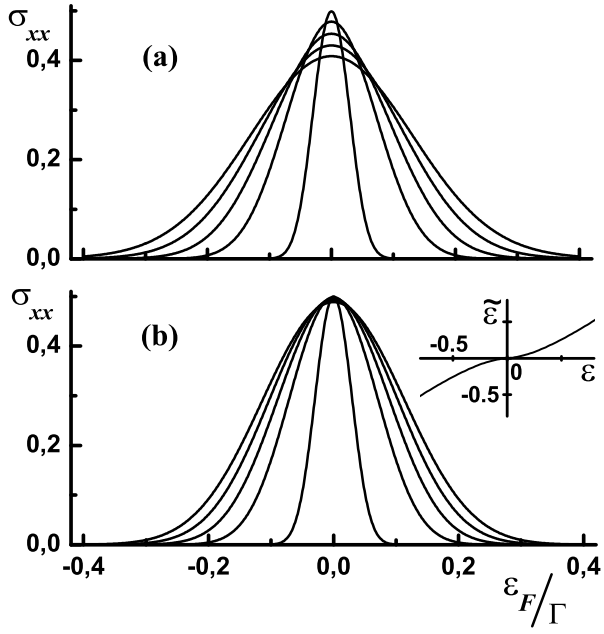

FIG. 4. Diagonal conductivity (in the units e^2/h), calculated from Eqs (23) and (26), is plotted vs. the dimensionless magnetic field ϵ_F/Γ for (a) $\tilde{\epsilon} = \epsilon$ (noninteracting electrons) and (b) for $\tilde{\epsilon}(\epsilon)$ shown in the inset. The curves are calculated for $T/\Gamma = 10^{-3}$ (lowest T), $T/\Gamma = 1.2 \cdot 10^{-2}$, $2.5 \cdot 10^{-2}$, $3.7 \cdot 10^{-2}$, $5 \cdot 10^{-2}$, respectively.

In the quantum Hall geometry, experimentally measured characteristics are the components, ρ_{xx} and ρ_{xy}, of the resistivity tensor, rather than σ_{xx}, σ_{xy}. The question how the dependence of σ_{xx} on the dimensionless magnetic field in Fig. 4 translates into the behavior of ρ_{xx} is by no means trivial. The common way to relate σ_{xx} and ρ_{xx} is to employ the semicircle law [11], i.e., $\rho_{xx} = 2\sigma_{xx}/\left[1 \pm (1 - 4\sigma_{xx}^2)^{1/2}\right]$. The underlying physics of the semicircle law is that the system is strongly inhomogeneous and represents a random mixture of the domains with quantized σ_{xy} and $\sigma_{xx} = 0$, while the macroscopic σ_{xx} the *portion* of the domains with $\sigma_{xy} = 1$ (left half of the semicircle) and $\sigma_{xy} = 0$ (right half of the semicircle). Therefore, in order for the semicircle relation to apply, we have to assume that $\sigma_{xx}(\epsilon_F)$, calculated above, represents, in fact, the average of the following distribution $f(\sigma) = \sigma_{xx}(\epsilon_F)\delta(\sigma) + (1 - \sigma_{xx}(\epsilon_F))\,\delta(1-\sigma)$. Obviously, Eq. (23) is valid for a homogeneous system. More specifically it implies that system parameters, e.g. the electron concentration, do not change within the spatial scale, L_ϕ. Formally this corresponds to the distribution $f^{(0)}(\sigma) = \delta(\sigma - \sigma_{xx})$. Both distributions f and $f^{(0)}$ have the same average. Whether or not macroscopic inhomogeneities (with a scale much bigger than L_ϕ) transform $f^{(0)}(\sigma)$ into $f(\sigma)$ depends on their magnitude. This magnitude should be neither very low (otherwise, they will only slightly smear $f^{(0)}(\sigma)$) nor very high (otherwise the distribution f will correspond to $\sigma_{xx} = 0.5$ with no sensitivity to ϵ_F). Assuming that the conditions for the semicircle rule are met, we immediately conclude that nondiagonal resistivity,

ρ_{xy}, is quantized at $\rho_{xy} = h/e^2$ for all $\sigma_{xx}(\epsilon_F)$ curves shown in Fig. 4b. This is the so called *quantum Hall insulator* behavior [18]. On the other hand, in the absence of $\mathcal{III}$, $\sigma_{xx} = 0.5$ only for the lowest temperature, as shown in Fig. 4a. Hence, no quantization of ρ_{xy}.

In this sense, $\mathcal{III}$ "reinforce" the metallic regime, and thus extend the quantum Hall insulator behavior to higher temperatures. Indeed, the dependence ρ_{xx} on the dimensionless magnetic field, calculated from Fig. 4b using the semicircle relation, and shown in Fig. 5 is close to the straight line in the logarithmic scale. The slope at high enough temperatures changes linearly with T and extrapolates to a nonzero value. However, we would like to point out that the temperature interval, in which this behavior takes place ($10^{-2}\Gamma < T < 5 \cdot 10^{-2}\Gamma$) is much narrower than in the experiment [17], where this behavior persisted as the temperature was raised by a factor of 30.

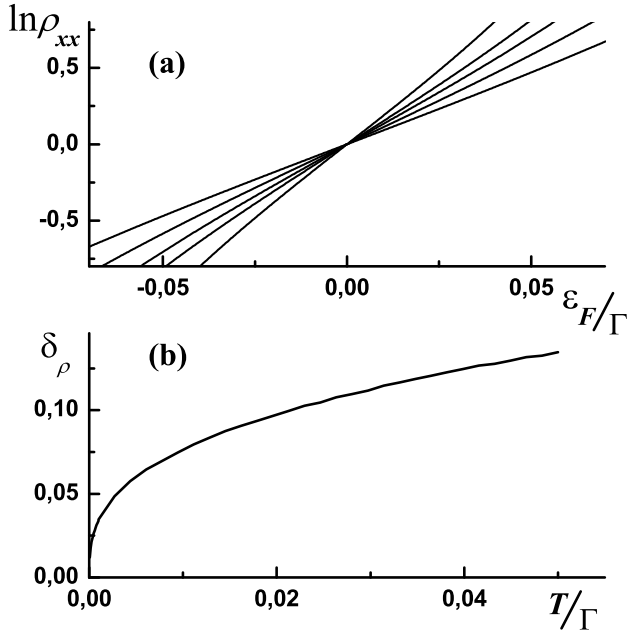

FIG. 5. (a) Diagonal resistivity is plotted in logarithmic scale as a function of dimensionless magnetic field, ϵ_F/Γ. The curves are calculated for $T/\Gamma = 10^{-3}$, 0.012, 0.025, 0.037, and 0.05. (b) The derivative $\delta_\rho = d \ln \rho_{xx}/d(\epsilon_F/\Gamma)$ at point $\epsilon_F = 0$ vs. dimensionless temperature, T/Γ.

V. Concluding Remarks

The most sound result of the present paper is the magnetic field dependence of σ_{xy} and σ_{xx} at low temperatures and strong enough interactions, Fig. 3. In particular, the rise of σ_{xy} from $\sigma_{xy} = 1$ to $\sigma_{xy} = 2$ (for *spinless* electrons) with *increasing* magnetic field seems counterintuitive. Indeed, σ_{xy} is the measure of the number of delocalized states below the Fermi level. Increasing magnetic field is supposed to facilitate localization. At the same time, the behavior of σ_{xy} shown in Fig. 3 reflects the fact that the $\mathcal{III}$ allows the emergence of additional delocalized states below the Fermi level as magnetic field increases. The reason for this counterintuitive behavior is the following. Exchange interactions modify, via $\mathcal{III}$, the strength of the electron scattering from the disorder potential. This modification is sensitive to the position of ϵ_F. As the Fermi level moves with magnetic field, the scattering of an electron with a given energy, ϵ, below ϵ_F changes, so that, at certain position of

ϵ_F, the delocalization condition, i.e., equal overall deflection to the left and to the right, is met for the energy ϵ.

We are not aware of any experiment in which the behavior depicted in Fig. 3 was observed directly. Recent observation [22] of a maximum in σ_{xy} at low magnetic fields can be loosely interpreted as interaction-induced creation of the additional delocalized states below ϵ_F.

Experimentally observed anomalous behavior of the components of the resistivity tensor in strong magnetic fields (quantum Hall insulator [18]) has spurred theoretical attempts to modify the standard microscopic description [1] of the quantum Hall effect. However, in previous considerations [19–21] additional delocalized states never emerged abruptly below ϵ_F. This is because these considerations assumed electrons to be either noninteractingzulicke or incoherent [19,20].

As we have demonstrated, there is a fundamental difference between the energy dependence of the $\mathcal{III}$ correction in one dimension [10] and in the quantum Hall geometry. In 1D, this correction is even in $(\epsilon - \epsilon_F)$, while in quantum Hall geometry it is an *odd* function of $(\epsilon - \epsilon_F)$. The underlying reason is the electron-hole symmetry, which we discuss below in more detail.

(i) The Hall conductivity can be calculated using the language of either electrons, $\sigma_{xy} = \sigma_{xy}^{(e)}$, or holes, $\sigma_{xy} = \sigma_{xy}^{(h)}$. The filling factor for holes is $1-\nu$, where ν is the filling factor for electrons. Even in the presence of interactions the condition $\sigma_{xy}^{(e)}(\nu) = \sigma_{xy}^{(h)}(1-\nu)$ should be obeyed. The fact that this condition is indeed obeyed within our consideration can be seen from Eqs. (20), (21). Changing ν by $(1-\nu)$ corresponds in to the replacement of ϵ_F by $-\epsilon_F$. Upon this replacement we get from Eq. (21) $Z \to -Z$. Then from Eq. (20) we get for the position of the delocalized state $\epsilon \to -\epsilon$. Thus, counting the delocalized states with the Fermi level $-\epsilon_F$, using the language of holes, yields the same number as for the Fermi level ϵ_F, using the language of electrons.

(ii) We turn to the different aspect of the e-h symmetry. It is generally assumed that there is a relation between the Hall conductivities of the 2D electron system in the lowest Landau level at filling factors ν and $(1-\nu)$

$$\sigma_{xy}(\nu) + \sigma_{xy}(1-\nu) = \frac{e^2}{h}. \tag{27}$$

This equation follows from the electron-hole symmetry and from the fact that the Hall conductivity of completely occupied Landau level is equal to e^2/h. In other words, Eq. (27) implies that there is only one delocalized state at any position of the Fermi level. It is easy to see that this relation is violated in our case. Indeed, at a magnetic field, at which there are two delocalized state below the Fermi level and one delocalized state above the Fermi level, the Hall conductivity of electrons is $\sigma_{xy}(\nu) = 2e^2/h$, while the Hall conductivity of holes is $\sigma_{xy}(1-\nu) = e^2/h$. Therefore, the sum of these two values yields $3e^2/h$, in contradiction to the r.h.s. of Eq. (27). Such inconsistency does not mean that our results violate the electron-hole symmetry. The reason for this is that r.h.s. of Eq. (27) should be calculated more carefully. Without interactions it is simply the conductivity of completely occupied Landau level, where the single-particle states, which are occupied by electrons, do not depend on the filling factor ν that enters Eq. (27). In the presence of interactions the situation is completely different . Again, the r.h.s. of Eq.(27) is the conductivity of completely occupied Landau level, but the single-particle states, which should be occupied in this case, strongly depend on the filling factor, ν. Strictly speaking, we should take the single-particle states of the electron system at filling factor ν and then, *considering them fixed*, add the electrons to all unoccupied states. Since in the example considered above, the "completely" occupied Landau band contains three delocalized states, such a counting yields the Hall conductivity $3e^2/h$. This suggests that Eq. (27) should be modified in the following way

$$\sigma_{xy}(\nu) + \sigma_{xy}(1-\nu) = \mathcal{N}_\nu \frac{e^2}{h}, \tag{28}$$

where $\mathcal{N}_\nu$ is the number of delocalized states in the lowest Landau level, when the electron filling factor is equal to ν.

Note finally, that the anomalous dependence $\mathcal{T}(\epsilon)$ in Fig. 2 emerges for the dimensionless interaction strength, α, defined by Eq. (16), exceeding the critical value. This result was obtained in the first order in α. If one attempts to incorporate higher order terms in α in the spirit of Ref. [10], then the second term in the r.h.s. of Eq. (13) would become singular in $(\epsilon - \epsilon_F)$. As a result the anomalous behavior of $\mathcal{T}(\epsilon)$ would persist for arbitrary small α.

We acknowledge the support of the NSF under grant No. INT-0231010. Interesting discussion with L.I. Glazman is gratefully acknowledged.

---

[1] J. T. Chalker and P. D. Coddington, J. Phys. C **21**, 2665 (1988).
[2] B. Shapiro, Phys. Rev. Lett. **48**, 823 (1982).
[3] D. Stauffer and A. Aharony, *Introduction to Percolation Theory* (Taylor and Francis, London, 1992).
[4] D.-H. Lee, Z. Wang, and S. Kivelson, Phys. Rev. Lett. **70**, 4130 (1993).
[5] B. Huckestein and R. Klesse, Phys. Rev. B **55**, R7303 (1997).
[6] Z. Wang, M. P. A. Fisher, S. M. Girvin, and J. T. Chalker, Phys. Rev. B **61**, 8326 (2000).
[7] D.-H. Lee and Z. Wang, Phys. Rev. Lett **76**, 4014 (1996).
[8] the studies of the effect of the long-range interaction on the transition are reviewed in B. Huckestein and M. Backhaus, ArXiv cond-mat/0004174 and references therein; see also Z. Wang and S. Xiong, Phys. Rev. B **65**, 195316 (2002), and references therein.
[9] B. L. Altshuler, A. G. Aronov, and D. E. Khmelnitsky, J. Phys. C **15**, 7367 (1982).
[10] K. A. Matveev, D. Yue, and L. I. Glazman, Phys. Rev. Lett. **71**, 3351 (1993); D. Yue, L. I. Glazman, and K. A. Matveev, Phys. Rev. B **49**, 1966 (1994).
[11] A. M. Dykhne and I. M. Ruzin, Phys. Rev. B **50**, 2369 (1994).
[12] I. Ruzin and S. Feng, Phys. Rev. Lett. **74**, 154 (1995).
[13] H. Fertig and B. I. Halperin, Phys. Rev. B **36**, 7969 (1987).
[14] L. P. Pryadko, E. Shimshoni, and A. Auerbach Phys. Rev. B **61**, 10929 (2000).
[15] S.-R. E. Yang, A. H. MacDonald, and B. Huckestein, Phys. Rev. Lett. **74**, 3229 (1995).
[16] Z. Wang and S. Xiong, Phys. Rev. B **65**, 195316 (2002), and references therein.
[17] D. Shahar, M. Hilke, C. C. Li, D. C. Tsui, S. L. Sondhi, and M. Razeghi, Solid State Commun. **107**, 19 (1998).
[18] D. Shahar, D. C. Tsui, M. Shayegan, E. Shimshoni, and S. L. Sondhi, Science **274**, 589 (1996).
[19] E. Shimshoni and A. Auerbach, Phys. Rev. B **55**, 9817 (1997).
[20] L. P. Pryadko and A. Auerbach, Phys. Rev. Lett. **82**, 1253 (1999).
[21] U. Zülicke and E. Shimshoni, Phys. Rev. B **63**, 241301 (2001).
[22] Z. D. Kwon, Y. Y. Proskuryakov, and A. K. Savchenko, ArXiv cond-mat/0301218.